International Journal of Quantum Information
Vol. 10, No. 2 (2012) 1250002 (11 pages)
© World Scientific Publishing Company
DOI: 10.1142/S0219749912500025

World Scientific
www.worldscientific.com

THE PHOTON-LIKE FLYING QUBIT IN THE COUPLED CAVITY ARRAY

MING-XIA HUO*, YING LI*, ZHI SONG*,‡ and CHANG-PU SUN*,†,§

*Department of Physics,
Nankai University — Tianjin 300071, China

†Institute of Theoretical Physics,
Chinese Academy of Sciences — Beijing 100080, China
‡songtc@nankai.edu.cn
§suncp@itp.ac.cn

Received 17 November 2011
Published 26 March 2012

We propose the simulation for an effective scheme to realize a spin network with tunable long-range couplings in the coupled cavity array with external multi-driving lasers. Via this scheme, the linear photon-like dispersion relation is achievable, which could be employed to perform a perfect quantum state transfer. Numerical results show that when applying two lasers in each cavity, the fidelity is higher than the highest fidelity of a classical transfer even for the transfer distance l increases up to 100 sites. In the simulation, as the number of lasers increases, the fidelity will be evidently enhanced for a wide range of l.

Keywords: Cavity; quantum state transfer; magnon.

Int. J. Quantum Inform. 2012.10. Downloaded from www.worldscientific.com
by CHINESE ACADEMY OF SCIENCES on 07/11/14. For personal use only.

1. Introduction

In many protocols of quantum information processing, it is highly desirable to perform a high-fidelity quantum state transfer (QST).[1–3] It was recognized that quantum spin lattices could be used as a data bus to transfer states without the need of conversion between different types of qubits.[1] In this data bus, the flying qubit is the photon-like[4–6], the magnon, which is an elementary excitation corresponding to the spin wave.[7] The main obstacle to perform a high-fidelity QST in quantum spin models is the spreading of the spin wave, which is due to the nonlinear dispersion relation. Some previous studies have shown that either the nonuniform nearest neighbor (NN) couplings[2,3,8,9] or the non-trivial long-range couplings[10,11] could be used to achieve the linear dispersion relation and perform a high-fidelity QST. Although with these developments, it is difficult to control the coupling distribution in quantum devices.

As recent developments, coupled cavity arrays have been intensively investigated in relation to their ability to realize and simulate quantum many body

Int. J. Quantum Inform. 2012.10. Downloaded from www.worldscientific.com
by CHINESE ACADEMY OF SCIENCES on 07/11/14. For personal use only.

phenomena.[12–19] In fact, the extremely high tunability, the individual addressability and the flexibility in their geometric design, make the coupled cavity arrays strong candidates for the realization of communication networks.

In this paper, using coupled cavity arrays with each cavity containing one three-level atom,[12] we realize spin models with tunable long-range couplings. For the coupled cavity systems, the photonic tunnelings induced long-range couplings between atoms could be optically tuned by external lasers. When tuning the couplings to achieve a linear photon-like dispersion relation, a perfect QST with high fidelity, long distance, and short time is achieved. Numerical results show that when applying two external lasers in each cavity, the fidelity is higher than the highest fidelity of a classical transfer even for the transfer distance increases up to 100 sites. As the number of lasers increases, the fidelity will be evidently enhanced for a wide range of the transfer distance. When the distance increases up to 500 sites, the fidelity could be always higher than 0.9 for 10 lasers and is almost close to unit and decays slightly for 14 lasers.

2. Model Setup

The considered model is a coupled cavity array with N cavities. Each cavity containing a Λ-level atom is driven by n_L external lasers (see Fig. 1(a)). The total Hamiltonian is

$$H = H_a + H_c + H_{ac} + H_{aL}, \tag{1}$$

where H_a describes Λ-level structure atoms, H_c describes photons in coupled cavities, H_{ac} represents the coupling between the cavity mode and atoms, and H_{aL} describes the coupling between atoms and n_L driving lasers.

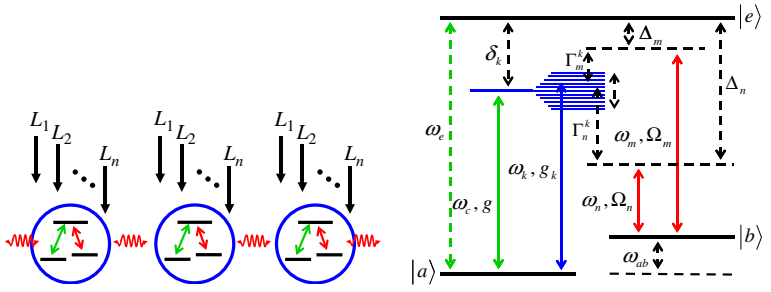

Fig. 1. (Color online.) Schematic diagram of Λ-type three-level atoms in coupled cavities. Each atom interacts with a single mode cavity and several external driving lasers. Levels $|a\rangle$, $|b\rangle$, and $|e\rangle$ have the energy values 0, ω_{ab}, and ω_e, respectively. The transition $|a\rangle \to |e\rangle$ is driven by photons with the frequency ω_c and interaction strength g. As a schematic diagram, we randomly choose and label only two possible driving lasers ω_n and ω_m with Rabi frequencies Ω_n and Ω_m. When cavities are coupled with each other, the degenerate cavity level ω_c becomes an energy band with bandwidth $2T$. Then the coupled cavity array is equivalent to a multi-mode cavity with frequencies ω_k. Γ_n^k and Γ_m^k equal to $\delta_k - \Delta_n$ and $\delta_k - \Delta_m$, respectively.

Such a system can be translational invariant, rather than that proposed in Refs. 2 and 3. So the operations in each cavity could be the same. The level structure of the atom trapped in each cavity is shown in Fig. 1(b), where the atom contains two long-lived states $|a\rangle$ and $|b\rangle$ and an excited state $|e\rangle$. For H_a, it can be written as

$$H_a = \sum_{j=1}^{N} (\omega_e |e\rangle_j \langle e| + \omega_{ab} |b\rangle_j \langle b|), \tag{2}$$

where the levels $|a\rangle$, $|b\rangle$, and $|e\rangle$ have the energy values 0, ω_{ab}, and ω_e, respectively. H_c describes photons as

$$H_c = \sum_{j=1}^{N} [\omega_c a_j^\dagger a_j - T(a_j^\dagger a_{j+1} + h.c.)], \tag{3}$$

where ω_c is the photonic frequency, T is the tunneling rate of photons between two neighboring cavities, and a_j ($a_j^\dagger$) annihilates (creates) a photon in cavity j. Here $a_{N+1} = a_1$ satisfies the periodic boundary condition. The transition between levels $|a\rangle$ and $|e\rangle$ is coupled to the cavity mode ω_c with the coupling g as

$$H_{ac} = \sum_{j=1}^{N} (g|e\rangle_j \langle a| a_j + h.c.), \tag{4}$$

and the transition between $|b\rangle$ and $|e\rangle$ is driven by n_L lasers $\{\omega_n\}$ with the Rabi frequency $\{\Omega_n\}$ as

$$H_{aL} = \frac{1}{2} \sum_{j=1}^{N} \sum_{n=1}^{n_L} (\Omega_n e^{-i\omega_n t} |e\rangle_j \langle b| + h.c.). \tag{5}$$

As a schematic diagram, in Fig. 1(b), we randomly choose and label only two possible driving lasers ω_n and ω_m with Rabi frequencies Ω_n and Ω_m. The difference $\omega_n - \omega_m$ is labeled as ω_{nm}, and the detunings are $\Delta_n = \omega_e - \omega_{ab} - \omega_n$ and $\Delta_m = \omega_e - \omega_{ab} - \omega_m$.

When considering the coupled cavity array as an even N site ring and taking the Fourier transformation

$$\tilde{a}_k^\dagger = \frac{1}{\sqrt{N}} \sum_{j=1}^{N} e^{ikj} a_j^\dagger, \tag{6}$$

the Hamiltonian H_c is diagonalized as

$$H_c = \sum_k \omega_k \tilde{a}_k^\dagger \tilde{a}_k = \sum_k (\omega_c - 2T \cos k) \tilde{a}_k^\dagger \tilde{a}_k, \tag{7}$$

where the momentum $k = 2j\pi/N$, $j = 0, 1, \ldots, N-1$. As shown in Fig. 1(b), two parameters are defined as $\delta_k = \omega_e - \omega_c + 2T \cos k$ and Γ_n^k (Γ_m^k) $= \delta_k - \Delta_n$ (Δ_m), where n (m) denotes the schematic driving laser with frequency ω_n (ω_m). Due to the

Int. J. Quantum Inform. 2012.10. Downloaded from www.worldscientific.com by CHINESE ACADEMY OF SCIENCES on 07/11/14. For personal use only.

tunneling of photons between neighboring cavities, the degenerate cavity level ω_c becomes an energy band with bandwidth $2T$. The transformation indicates that the coupled cavity array is equivalent to a multi-mode cavity with frequencies ω_k, which makes it possible to realize effective long-range couplings between two atoms placed in distant cavities.

3. Adiabatic Elimination of Atomic and Photonic Excited States

Consider the case that each driving laser contributes to the effective Hamiltonian independently. To adiabatically eliminate the atomic excited states $|e\rangle$ and photonic states, the photon excitations should be strongly suppressed and the virtual photon emitted by the atom should be always absorbed by other atoms. It requires that for any $k \in [0, 2\pi)$ and any $n \in [1, n_L]$,

$$|\delta_k|, |\Delta_n| \gg |g|, |\Omega_m|, |\Gamma^{k'}_m|, |\omega_{lm}| \tag{8}$$

and

$$|\Gamma^k_n|, |\omega_{nm}| \gg \left|\frac{g\Omega_l}{\Delta_l}\right|, \left|\frac{\Omega_l^2}{\Delta_l}\right| \tag{9}$$

for any $k' \in [0, 2\pi)$ and any $m, l \in [1, n_L]$. The first condition in Eq. (8) suppresses the excitation of the atomic excited states $|e\rangle$, while the second condition in Eq. (9) suppresses the photonic excitations and guarantees that each driving laser is independent.

Now turn to the interaction picture with

$$H_0 = H_a + H_c \tag{10}$$

and

$$\begin{aligned} H_1 &= e^{iH_0t}(H_{ac} + H_{aL})e^{-iH_0t} \\ &= \sum_{j=1}^{N} |e\rangle_j\langle a| \sum_k \frac{g}{\sqrt{N}} e^{i(kj+\delta_k t)}\tilde{a}_k + \frac{1}{2}\sum_{n=1}^{n_L} \Omega_n e^{i\Delta_n t}|e\rangle_j\langle b| + h.c. \end{aligned} \tag{11}$$

Through adiabatically eliminating the atomic excited state and ignoring the high-frequency terms, the effective Hamiltonian of H_1 becomes

$$\begin{aligned} H_2 &= -iH_1(t)\int_{-\infty}^{t} dt' H_1(t') \\ &= -\sum_{j,k}[\mathcal{G}_j(k,t)\sigma_+^{(j)}\tilde{a}_k + h.c.], \end{aligned} \tag{12}$$

where the pseudo spin operators are

$$\begin{aligned} \sigma_z^{(j)} &= |b\rangle_j\langle b| - |a\rangle_j\langle a|, \\ \sigma_+^{(j)} &= |b\rangle_j\langle a|, \end{aligned} \tag{13}$$

Int. J. Quantum Inform. 2012.10. Downloaded from www.worldscientific.com
by CHINESE ACADEMY OF SCIENCES on 07/11/14. For personal use only.

and the coefficient

$$\mathcal{G}_j(k,t) = \frac{g}{\sqrt{N}} \sum_n \frac{\Omega_n^*}{2\Delta_n} e^{i(kj+\Gamma_n^k t)}. \tag{14}$$

Note that the Hamiltonian (12) is equivalent to the Jaynes Cummings model which describes the interaction of a single, quasi-resonant optical cavity field with a two-level atom.[20]

Eliminating the photonic degree of freedom and considering that for the studied state $\langle a_k^\dagger a_{k'} \rangle \ll 1$ and $\langle a_k a_{k'} \rangle = 0$, we have

$$\begin{aligned} H_3 &= -iH_2(t) \int_{-\infty}^{t} dt' H_2(t') \\ &= -\sum_{j,j'} \sum_{n=1}^{n_L} \left| \frac{g\Omega_n}{2\Delta_n} \right|^2 S_{j,j'}^{[n]} \sigma_+^{(j)} \sigma_-^{(j')}, \end{aligned} \tag{15}$$

where

$$S_{j,j'}^{[n]} = \frac{1}{N} \sum_k \frac{e^{ik(j-j')}}{\mathcal{D}_n - 2T\cos k} \tag{16}$$

and

$$\mathcal{D}_n = \omega_c - \omega_{ab} - \omega_n. \tag{17}$$

For each item of $S_{j,j'}^{[n]}$ in (16), the imaginary part with k is opposite to that with $k+\pi$. Then after the sum of k from 0 to 2π, all of the imaginary parts are eliminated. Therefore, $S_{j,j'}^{[n]}$ is always real. Combining H_0, the effective Hamiltonian of atoms is obtained as

$$H_{\text{eff}} = -\sum_{j,j'} \frac{J_{j,j'}}{2} \left(\sigma_+^{(j)} \sigma_-^{(j')} + h.c. \right) + \sum_{j=1}^{N} \frac{\omega_{ab}}{2} \sigma_z^{(j)}, \tag{18}$$

where

$$J_{j,j'} = \sum_{n=1}^{n_L} \left| \frac{g\Omega_n}{2\Delta_n} \right|^2 S_{j,j'}^{[n]}. \tag{19}$$

It is a standard XY model with tunable long-range couplings and $J_{j,j'} = J_{j',j} = J(|j-j'|)$.

In the following two limits, Eq. (16) could be simplified. First, in the narrow band limit $|\mathcal{D}_n| \gg |2T|$, Eq. (16) becomes

$$S_{j,j'}^{[n]} \simeq \delta_{j,j'} \frac{1}{\mathcal{D}_n} + \delta_{|j-j'|,1} \frac{T}{\mathcal{D}_n^2}, \tag{20}$$

which is reduced to the result of the spin model with NN couplings obtained in Ref. 12. In this model, the dispersion relation is cosinusoidal, which is quadratic for

Int. J. Quantum Inform. 2012.10. Downloaded from www.worldscientific.com by CHINESE ACADEMY OF SCIENCES on 07/11/14. For personal use only.

small momenta and linear around $k = \pm\pi/2$.[6,21] In the other limit $N \to \infty$, it becomes

$$S_{j,j'}^{[n]} = \eta_n^{j-j'+1} \frac{1}{\sqrt{\mathcal{D}_n^2 - 4T^2}} \exp\left(-\frac{|j-j'|}{\xi_n}\right), \tag{21}$$

where $\eta_n = \text{sign}\,(\mathcal{D}_n/T)$ and ξ_n is the characteristic length of the effective long-range couplings with

$$\xi_n^{-1} = -\ln\left[\left|\frac{\mathcal{D}_n}{2T}\right| - \sqrt{\left(\frac{\mathcal{D}_n}{2T}\right)^2 - 1}\right]. \tag{22}$$

Here, the Stark effect and an irrelevant constant have been dropped. In fact, the order of magnitude of the Stark effect is about Ω^2/Δ, which is much less than Γ under the considered condition in Eq. (9). According to Eq. (16), its contribution to the final result should be much less than the effective coupling J.

4. The High Efficiency QST

For a standard XY model, the Hamiltonian is

$$H_{XY} = -\sum_{j,l} \frac{J(l)}{2}\left(\sigma_+^{(j)}\sigma_-^{(j+l)} + h.c.\right), \tag{23}$$

where the coupling constants $J(l) = J(-l)$. The eigenstates in the subspace with a single spin flipped on a ferromagnetic background are defined as

$$|k\rangle = 1/\sqrt{N}\sum_{j=1}^{N} e^{ikj}|j\rangle, \tag{24}$$

where

$$|j\rangle = \sigma_+^{(j)} \prod_{j'=1}^{N} |\downarrow\rangle_{j'}. \tag{25}$$

The spin-down state $|\Downarrow\rangle$ represents the ground state of the pseudo spin.

The dispersion relation for a single magnon is

$$E_k = -J(0) - \sum_{l>0} 2J(l)\cos kl, \tag{26}$$

and for the linear dispersion relation $E_k = |k|$, the corresponding Fourier expansion is

$$E_k = \frac{\pi}{2} - \frac{2}{\pi}\sum_{l=1}^{\infty} \frac{1-(-1)^l}{l^2}\cos lk, \tag{27}$$

Int. J. Quantum Inform. 2012.10. Downloaded from www.worldscientific.com by CHINESE ACADEMY OF SCIENCES on 07/11/14. For personal use only.

Int. J. Quantum Inform. 2012.10. Downloaded from www.worldscientific.com
by CHINESE ACADEMY OF SCIENCES on 07/11/14. For personal use only.

which requires

$$J(0) = -\frac{\pi}{2}, J(l \neq 0) = \frac{1-(-1)^l}{\pi l^2}. \tag{28}$$

There are two characters in the coupling constant distribution: the odd-modulation by factor $1-(-1)^l$ and inverse-square decay. In fact, to achieve the odd-modulation coupling distribution, one can group the driving lasers into $n_L/2$ pairs with each pair obeying

$$\begin{aligned} \left|\frac{\Omega_{2m-1}}{\Delta_{2m-1}}\right| &= \left|\frac{\Omega_{2m}}{\Delta_{2m}}\right| = G_{2m}, \\ \mathcal{D}_{2m-1} &= -\mathcal{D}_{2m}, \in [1, n_L/2], \end{aligned} \tag{29}$$

which leads to the coupling distribution

$$J_{j,j'} = \frac{g^2}{4}\sum_{m=1}^{n_L/2} G_{2m}^2 \left| S_{j,j'}^{[2m]} \right| [1-(-1)^{j-j'}]. \tag{30}$$

On the other hand, the inverse-square decay is realizable via choosing D_n and G_n. For systems with $n_L = 2, 4, \ldots,$ and 14, numerical calculations are performed to search optimal parameters D_n and G_n ($n \in [1,n_L]$) to get the precise inverse-square decay of the coupling distribution. The optimal parameters are listed in Table 1. Correspondingly, the distribution of coupling strengths $J(l)$ is displayed in Table 2 in unit $J(1)$. With n_L lasers, the first $n_L/2+1$ coupling strengths can always be

Table 1. Parameters D_n in unit T, and G_n in unit G_2 ($n \in [1, n_L]$) obtained from numerical simulations for the optimal setups with $n_L = 2, 4, \ldots,$ and 14. Based on these parameters, the corresponding dispersion relations (Fig. 2), coupling constant distributions (Table 2), and fidelities of the QST (Fig. 3) are obtained.

	n_L	$n=2$	4	6	8	10	12	14
	2	3.333						
	4	5.200	2.121					
	6	10.100	7.212	2.226				
$\frac{D_n}{T}$	8	10.100	7.212	3.633	2.090			
	10	10.100	7.212	5.947	2.395	2.027		
	12	10.100	7.212	5.947	4.044	2.333	2.023	
	14	10.100	7.212	5.947	4.327	2.565	2.085	2.006
	2	1						
	4	1	0.044					
	6	1	0.351	0.084				
$\frac{G_n}{G_2}$	8	1	1.096	0.548	0.085			
	10	1	0.535	0.926	0.177	0.030		
	12	1	1.013	0.333	0.359	0.155	0.026	
	14	1	0.429	0.234	0.218	0.138	0.037	0.006

Table 2. The coupling constant distributions $J(l)/J(1)$ obtained from optimal parameters for $n_L = 2, 4, \ldots,$ and 14 in Table 1 and compared to the ideal distributions (28). It is found that for a given n_L, the first $n_L/2+1$ coupling strengths are always equal to those of the ideal distribution. For $l > n_L/2+1$, couplings $J(l)/J(1)$ are always less than the ideal ones, $1/l^2$. It is indicated that the truncated ideal coupling distribution can be achievable by applying optimal n_L lasers.

l	$n_L = 2$	4	6	8	10	12	14	ideal
1	$\frac{1}{1^2}$	$\frac{1}{1^2}$	$\frac{1}{1^2}$	$\frac{1}{1^2}$	$\frac{1}{1^2}$	$\frac{1}{1^2}$	$\frac{1}{1^2}$	$\frac{1}{1^2}$
3	$\frac{1}{3.0^2}$	$\frac{1}{3.0^2}$	$\frac{1}{3^2}$	$\frac{1}{3^2}$	$\frac{1}{3^2}$	$\frac{1}{3^2}$	$\frac{1}{3^2}$	$\frac{1}{3^2}$
5	$\frac{1}{9.0^2}$	$\frac{1}{5.0^2}$	$\frac{1}{5^2}$	$\frac{1}{5^2}$	$\frac{1}{5^2}$	$\frac{1}{5^2}$	$\frac{1}{5^2}$	$\frac{1}{5^2}$
7	$\frac{1}{27.0^2}$	$\frac{1}{8.4^2}$	$\frac{1}{8.0^2}$	$\frac{1}{7^2}$	$\frac{1}{7^2}$	$\frac{1}{7^2}$	$\frac{1}{7^2}$	$\frac{1}{7^2}$
9	$\frac{1}{80.7^2}$	$\frac{1}{13.9^2}$	$\frac{1}{12.8^2}$	$\frac{1}{9.5^2}$	$\frac{1}{9^2}$	$\frac{1}{9^2}$	$\frac{1}{9^2}$	$\frac{1}{9^2}$
11	$\frac{1}{234.5^2}$	$\frac{1}{23.2^2}$	$\frac{1}{20.6^2}$	$\frac{1}{12.8^2}$	$\frac{1}{11.0^2}$	$\frac{1}{11^2}$	$\frac{1}{11^2}$	$\frac{1}{11^2}$
13	$\frac{1}{565.1^2}$	$\frac{1}{38.7^2}$	$\frac{1}{32.9^2}$	$\frac{1}{17.3^2}$	$\frac{1}{13.2^2}$	$\frac{1}{13.1^2}$	$\frac{1}{13^2}$	$\frac{1}{13^2}$
15	$\frac{1}{827.9^2}$	$\frac{1}{64.5^2}$	$\frac{1}{52.7^2}$	$\frac{1}{23.3^2}$	$\frac{1}{15.7^2}$	$\frac{1}{15.4^2}$	$\frac{1}{15.0^2}$	$\frac{1}{15^2}$
17	$\frac{1}{886.2^2}$	$\frac{1}{107.4^2}$	$\frac{1}{84.4^2}$	$\frac{1}{31.4^2}$	$\frac{1}{18.6^2}$	$\frac{1}{18.0^2}$	$\frac{1}{17.0^2}$	$\frac{1}{17^2}$
19	$\frac{1}{893.5^2}$	$\frac{1}{179.1^2}$	$\frac{1}{135.2^2}$	$\frac{1}{42.4^2}$	$\frac{1}{21.9^2}$	$\frac{1}{20.9^2}$	$\frac{1}{18.9^2}$	$\frac{1}{19^2}$

modulated to the corresponding ideal distribution, and the rest $J(l)$ $(l > n_L/2+1)$ are smaller than the ideal ones, i.e. $J(l)/J(1) < 1/l^2$.

It seems that infinite lasers may be required to get a precise distribution as shown in (28). However, because the contribution of $J(l)$ to E_k reduces fast as l increases due to its inverse-square decay, the linear dispersion relation is achievable approximately with several lasers. To demonstrate this, we study the systems with $n_L = 2$ and 4. The corresponding dispersion curves and group velocities are plotted in Fig. 2 and compared to those of the ideal case. The obtained results indicate that the linear dispersion relation is achievable approximately with $n_L = 2$ and 4.

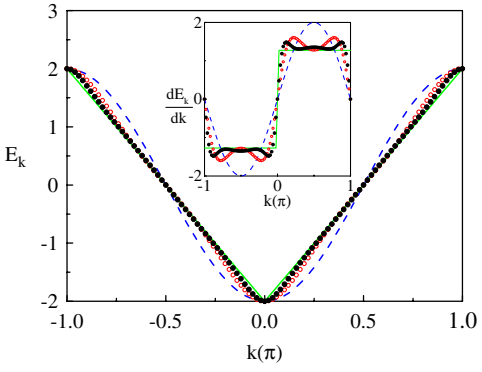

Fig. 2. (Color online.) Dispersion curves of single magnon in systems with different coupling distributions for $n_L = 2$ (empty circle), $n_L = 4$ (solid circle), and the ideal case $E_k = |k|$ (solid line), as given in Table 2. The dash line corresponds to the one with uniform nearest-neighbor couplings. The inset shows the derivatives (group velocities) of dispersion curves. It is indicated that the photon-like dispersion relation is achievable approximately via the application of external lasers.

Int. J. Quantum Inform. 2012.10. Downloaded from www.worldscientific.com
by CHINESE ACADEMY OF SCIENCES on 07/11/14. For personal use only.

Next we apply the analysis to the QST in a N-site ring. The quantum state to be transferred at an arbitrary site N_0 has the form[1]

$$|\psi(N_0)\rangle = \left[\cos\frac{\theta}{2} + e^{i\varphi}\sin\frac{\theta}{2}\sigma_+^{(N_0)}\right]\prod_{j'=1}^{N}|\downarrow\rangle_{j'}. \tag{31}$$

In a coupled cavity system, $|\psi(j)\rangle$ denotes that the atomic state in the jth cavity is $\cos(\theta/2)|a\rangle + e^{i\varphi}\sin(\theta/2)|b\rangle$, while all the atoms in other cavities are in the state $|a\rangle$. In the ideal case, this state can be perfectly transferred to site $N_0 + N/2$ after a period of time $\tau = N\pi/2W$, where W is the width of the energy band, which is dependent on g as $W \propto g^2$.

To illustrate the efficiency of our scheme, we simulate a QST in N-site systems with optimal coupling distributions for $n_L = 2, 4, \ldots,$ and 14 as listed in Table 2. Initially, we set the quantum state to be transferred at site N_0. The initial state can be written as $|\psi(N_0)\rangle$. In order to compare with the results obtained in a uniform spin chain,[1] we adopt the average fidelity (hereafter referred to as fidelity) in the form

$$F(t) = \frac{|f(t)|}{3} + \frac{|f(t)|^2}{6} + \frac{1}{2}, \tag{32}$$

to character the efficiency of QST, where the transition amplitude of a magnon from site N_0 to $N_0 + N/2$ is

$$f(t) = \langle\psi(N_0 + N/2)|e^{-iHt}|\psi(N_0)\rangle. \tag{33}$$

In Fig. 3, the fidelity $F = \max F(t)$ with $t \sim \tau$ as a function of N is plotted with parameters listed in Table 1. As an example, for $n_L = 6$, the parameters $\Delta_1 = 21\,\text{GHz}$, $g = 1\,\text{GHz}$, $\Omega_1 = 2\,\text{GHz}$, and $D_1 = 1$ GHz. Using these parameters, all the parameters are obtainable via Table 1. The dash line of $F = 2/3$ shows the highest fidelity for a classical transfer.[1,22] The fidelity obtained in our scheme with $n_L = 2$ is higher than that of a classical transfer even for the transfer distance increases up to $N/2 = 100$ sites. As the number of lasers increases, the fidelity will be evidently enhanced for a wide range of the transfer distance. When the distance increases up to 500 sites, the fidelity could be always higher than 0.9 for 10 lasers and is almost close to unit with slight decay for 14 lasers.

The decoherence of the system mainly results from the decay mechanisms via the photons or the excited state of atoms. Such an environmental effect may induce errors on the transmitted state. In our scheme, under the condition of the adiabatic elimination, the occupation of the atomic excited state $|e\rangle$ and the number of photons are small. Moreover, we consider the strong coupling regime, where the photon−atom coupling g is much larger than the spontaneous emission rate and the cavity decay rate. To perform a high efficiency QST that sufficiently exceeds the decay rates, atom−photon couplings should exceed cavity decay rates. Promising

Int. J. Quantum Inform. 2012.10. Downloaded from www.worldscientific.com
by CHINESE ACADEMY OF SCIENCES on 07/11/14. For personal use only.

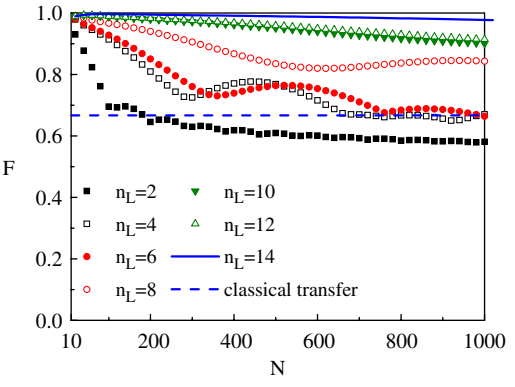

Fig. 3. (Color online.) The fidelity as a function of N for systems with different n_L. Parameters are set as listed in Table 1. As an example, for $n_L = 6$, the parameters are $\Delta_1 = 21\,\text{GHz}$, $g = 1\,\text{GHz}$, $\Omega_1 = 2\,\text{GHz}$, and $D_1 = 1\,\text{GHz}$. Using these parameters, all the parameters are obtainable via Table 1. The dash line of $F = 2/3$ denotes the highest fidelity of a classical transfer. With $n_L = 2$, the fidelity obtained in our scheme is higher than that of a classical transfer even for the transfer distance increases up to $N/2 = 100$ sites. Moreover, the fidelity F gets better as n_L increases. When the distance increases up to 500 sites, the fidelity is always higher than 0.9 for 10 lasers and almost close to unit with slight decay for 14 lasers.

candidates for an implementation are therefore toroidal microcavities with a very large Q factor which is larger than 10^8. It can be produced in large numbers, addressing with high precision, and efficiently coupled to optical fibers as well as to Cs atoms.[16] Photonic crystals are also good candidates. The nanocavities based on photonic crystals offer the possibility for the fabrication of large arrays of cavities in lattices or networks.[23–26] Circuit cavities interacting with a Cooper pair box would have very low cavity decay with $Q \sim 10^6$ if engineered in a row.[27] Also they are suitable for an implementation. In our scheme, the fidelity is higher than that of a classical transfer even for the transfer distance increases up to 100 sites with two lasers. The well-known Electromagnetically Induced Transparency phenomenon occurs in systems where three-level atoms are coupled to two lasers.[28,29]

To overcome the decoherence, the coefficients of the effective model should be much larger than the effective decay rates of the photons and the atomic spontaneous emission. With the considered parameters in our scheme, the coupling constant $J(l)$ is equal to $\frac{1}{1600}\,\text{GHz}$. The probabilities of photonic and atomic excitations are both $\frac{1}{400}$. Therefore, our scheme requires that the decay rate of the atomic excited states and the cavity loss rate are smaller than $5 \times 10^{-4}\,\text{GHz}$, which is available in experiments.[12]

5. Summary

In conclusion, we proposed an effective scheme to realize a spin network with tunable long-range couplings in the coupled cavity array with external multi-driving lasers. For the coupled cavity systems with each cavity containing one three-level

Int. J. Quantum Inform. 2012.10. Downloaded from www.worldscientific.com by CHINESE ACADEMY OF SCIENCES on 07/11/14. For personal use only.

atom, the photonic tunnelings induced long-range couplings between atoms could be optically tuned by external lasers. Then it is possible to pre-engineer a standard XY spin model and achieve a linear photon-like dispersion relation for the magnon, which could be employed to perform a high-fidelity QST. Numerical results show that when applying two lasers in each cavity, the fidelity is higher than the highest fidelity of a classical transfer even for the transfer distance increases up to 100 sites. As the number of lasers increases, the fidelity is evidently enhanced for a wide range of the transfer distance.

Acknowledgments

We acknowledge the support of the CNSF (Grant No. 10874091) and National Basic Research Program (973 Program) of China under Grant No. 2012CB921900.

Int. J. Quantum Inform. 2012.10. Downloaded from www.worldscientific.com by CHINESE ACADEMY OF SCIENCES on 07/11/14. For personal use only.

References

1. S. Bose, *Phys. Rev. Lett.* **91** (2003) 207901.
2. M. Christandl, N. Datta, A. Ekert and A. J. Landahl, *Phys. Rev. Lett.* **92** (2004) 187902.
3. M. Christandl *et al.*, *Phys. Rev. A* **71** (2005) 032312.
4. J. I. Cirac, P. Zoller, H. J. Kimble and H. Mabuchi, *Phys. Rev. Lett.* **78** (1997) 3221.
5. T. J. Osborne and N. Linden, *Phys. Rev. A* **69** (2004) 052315.
6. S. Yang, Z. Song and C. P. Sun, *Phys. Rev. A* **73** (2006) 022317.
7. D. P. DiVincenzo, *Fortschr. Phys.* **48** (2000) 9.
8. M. H. Yung and S. Bose, *Phys. Rev. A* **71** (2005) 032310.
9. T. Shi, Y. Li, Z. Song and C. P. Sun, *Phys. Rev. A* **71** (2005) 032309.
10. A. Kay, *Phys. Rev. A* **73** (2006) 032306.
11. M. Avellino, A. J. Fisher and S. Bose, *Phys. Rev. A* **74** (2006) 012321.
12. M. J. Hartmann, F. G. S. L. Brandão and M. B. Plenio, *Phys. Rev. Lett.* **99** (2007) 160501.
13. A. D. Greentree, C. Tahan, J. H. Cole and L. C. L. Hollenberg, *Nature Phys.* **2** (2006) 856.
14. M. J. Hartmann, F. G. S. L. Brandão and M. B. Plenio, *Nature Phys.* **2** (2006) 849.
15. M. J. Hartmann and M. B. Plenio, *Phys. Rev. Lett.* **99** (2007) 103601.
16. D. K. Armani, T. J. Kippenberg, S. M. Spillane and K. J. Vahala, *Nature* **421** (2003) 925.
17. T. Aoki *et al.*, *Nature* **443** (2006) 671.
18. S. M. Spillane *et al.*, *Phys. Rev. A* **71** (2005) 013817.
19. D. G. Angelakis, M. F. Santos and S. Bose, *Phys. Rev. A* **76** (2007) 031805(R).
20. E. T. Jaynes and F. W. Cummings, *Proc. IEEE* **51** (1963) 89.
21. B. Chen, Z. Song and C. P. Sun, *Phys. Rev. A* **75** (2007) 012113.
22. M. Horodecki, P. Horodecki and R. Horodecki, *Phys. Rev. A* **60** (1999) 1888.
23. Y. Akahane, T. Asano, B. S. Song and S. Noda, *Nature* **425** (2003) 944.
24. B. S. Song, S. Noda, T. Asano and Y. Akahane, *Nature Mater.* **4** (2005) 207.
25. A. Badolato *et al.*, *Science* **308** (2005) 1158.
26. P. E. Barclay, K. M. Fu, C. Santori and R. G. Beausoleil, *Opt. Express* **17** (2009) 9588.
27. A. Wallraff *et al.*, *Nature* **431** (2004) 162.
28. M. Fleischhauer, A. Imamoğlu and J. P. Marangos, *Rev. Mod. Phys.* **77** (2005) 633.
29. M. Arikawa *et al.*, *Phys. Rev. A* **81** (2010) 021605(R).